

# METIS-SPECS: DECOUPLING LEARNING VIA SELF-DISTILLED PREFERENCE-BASED COLD START FOR VLMS

Kun Chen<sup>1,2,\*</sup>, Peng Shi<sup>3,\*</sup>, Haibo Qiu<sup>3</sup>, Zhixiong Zeng<sup>3</sup>, Siqi Yang<sup>3</sup>, Wenji Mao<sup>2,1,†</sup>, Lin Ma<sup>3,†</sup>

<sup>1</sup>School of Artificial Intelligence, University of Chinese Academy of Sciences

<sup>2</sup>MAIS, Institute of Automation, Chinese Academy of Sciences

<sup>3</sup>Meituan

chenkun2024@ia.ac.cn shipeng10@meituan.com

wenji.mao@ia.ac.cn forest.linma@gmail.com

## ABSTRACT

Reinforcement learning (RL) with verifiable rewards has recently catalyzed a wave of “MLLM-r1” approaches that bring RL to vision language models. Most representative paradigms begin with a cold start, typically employing supervised fine-tuning (SFT), to initialize the policy before RL. However, SFT-based cold start adopts the reasoning paradigm intertwined with task solution and output format, which may induce instruction-style overfitting, weakens out-of-distribution generalization, and ultimately affects downstream RL. We revisit the cold start along two views, its training method and data construction, and introduce the *Generalization Factor* (GF) coefficient to quantify the generalization capability under different methods. Our empirical study finds that preference-based training methods (e.g. DPO) generalizes better than SFT-based methods in cold start. Motivated by this, we propose **SPECS**—a Self-distilled, Preference-based Cold Start framework that decouples multimodal learning: (1) generates introspective preference data pairs via self-distillation, avoiding reliance on larger teachers or manual annotation; (2) performs preference-based training to learn, focusing on shallow, transferable surface-form criteria (format, structure, style) rather than memorizing content; and (3) hands off to RL with verifiable rewards for deep reasoning results. Experimental results across multiple multimodal benchmarks show that our decoupling learning framework yields consistent performance gains over strong baselines, improving MEGA-BENCH by 4.1% and MATHVISTA by 12.2%. Additional experiments indicate that SPECS contributes to reducing in-distribution “stuckness,” improving exploration, stabilizing training, and raising the performance ceiling.<sup>1</sup>

## 1 INTRODUCTION

Recently, inspired by the success of DeepSeek-R1 (Guo et al., 2025), in effectively enhancing the reasoning capabilities of large models through reinforcement learning (RL) with verifiable reward (Lambert et al., 2024; Guo et al., 2025), a growing body of work has begun to apply RL directly to vision language models (VLMS). This has led to a wave of exciting “MLLM-r1” research (Meng et al., 2025; Shen et al., 2025; Peng et al., 2025; Zhou et al., 2025; Zhang et al., 2025a; Wang et al., 2025b;a; Zheng et al., 2025; Ma et al., 2025), which leverage similar principles to advance multimodal reasoning.

Previous research has indicated that prior to RL, employing a pre-training or warm-up phase (which is termed “**cold start**”), can significantly improve the readability, stability, and even the final performance of RL training (Guo et al., 2025). Currently, the most commonly used cold start strategy

---

\*Equal contribution. †Corresponding author(s).

<sup>1</sup>Project Page: <https://github.com/Kwen-Chen/SPECS-VL>

is supervised fine-tuning (SFT), where the model is first fine-tuned on a set of high-quality Chain-of-Thought reasoning data to provide a better initial policy for the subsequent RL phase (Wei et al., 2025; Yang et al., 2025; Huang et al., 2025; Deng et al., 2025b). This strategy enables the model to be trained on complex reasoning data during the cold start phase, thereby acquiring reasoning ability.

The common understanding behind SFT-based cold start is that reasoning abilities, reasoning format and other learning objectives can be jointly learned during the cold start phase. However, such an SFT-based joint learning paradigm may largely affect the model’s generalization capability (Wu et al., 2025; Chu et al., 2025), and consequently degrade subsequent RL (Chen et al., 2025a). This raises an important research issue of quantifying and improving the model’s *generalization capability* during cold start and working in concert with subsequent RL.

To address the above limitations, we consider an alternative learning paradigm, which separates the learning process into hierarchical stages based on the idea that cold start phase focused more on shallow, surface-form learning to avoid prematurely getting stuck in in-distribution problem solving, while subsequent RL focuses on the deep-level learning of a solution to boost the overall performance (Bengio et al., 2009). Thus, the intuition of our adopting decoupling learning for multimodal reasoning is that the selection of pre-training methods in cold start needs to better support the subsequent RL, both in terms of generalization and by having separate objectives to facilitate better final results.

Another important issue is the generation of cold start data. Previously, the prohibitive cost of human annotation has motivated a growing body of research to explore the use of synthetic data. This often involves using a more capable large model as a “teacher” to distill data for a smaller “student” model. (Zhang et al., 2025b; Yao et al., 2024; Xu et al., 2024; Huang et al., 2025). However, when the capability gap between the teacher model and the student model is too large, it can lead to a decline in model performance (Zhang et al., 2023). Alternatively, the DeepSeek-R1-Zero paradigm (Guo et al., 2025) first directly applies reinforcement learning to the base model for obtaining R1-Zero and then generates cold start data by zero model itself. This paradigm has achieved very remarkable performance; yet it still has the limitation of reliance on the SFT cold start and the constraints between SFT and subsequent RL, thereby leaving room for further improvement.

In this paper, to examine the suitable cold start training method, we propose the *Generalization Factor* (GF) coefficient in Section 2 to quantify the generalization capability of the model and conduct an empirical study to evaluate different training methods. We identify that Direct Preference Optimization (DPO) (Rafailov et al., 2023) based on preference data is a cold start approach that enables the model to have better performance. On this basis, we present the Self-distilled Preference-based Cold-Start (SPECS) framework in Section 3. By decoupling the learning objectives during DPO to focus on output format, we create a pre-aligned model that serves as a superior starting point for the final RL fine-tuning. Our experiments show that this method leads to more stable, efficient training, and a higher performance ceiling compared to the advanced and strong baseline.

The main contributions of this paper can be summarized as follows.

1. We present the **SPECS** framework, a three-stage cold start strategy. It generates preference data through self-distillation, uses DPO for cold start training, and separates training objectives so that the model first aligns with output formats, providing a stronger starting point for RL.
2. We propose **Generalization Factor** as a metric to evaluate a model’s generalization capability under different cold start training methods by comparing its performance on in-distribution and out-of-distribution tasks.
3. We reveal the importance of **Decoupling Learning** between the cold-start and RL phases. This separation improves exploration and reduces the risk of the model getting stuck on in-distribution solutions.
4. Our experimental results prove that a preference-based DPO cold start gives the model stronger generalization ability. In terms of the model’s final results, it achieves consistent performance gains across benchmarks, improving MEGA-Bench by 4.1% and MathVista by 12.2% over strong baselines, demonstrating the effectiveness of the SPECS.

## 2 EMPIRICAL INVESTIGATION

### 2.1 EVALUATING DEGREE OF GENERALIZATION

To evaluate the impact of preference-based versus supervised data on a model’s generalization capabilities under a fixed sample size, we introduce the metric of **Generalization Factor (GF)**.

**Setup.** We define an evaluation function  $\psi(f, P) \in \mathbb{R}$  that measures the performance of a model  $f$  on a data distribution  $P$ . A higher value of  $\psi$  indicates better performance.

We consider two types of training data, denoted by  $\tau \in \{\text{pref}, \text{sup}\}$ , corresponding to preference data and supervised data. For a given data type  $\tau$  and a fixed sample size  $n$ , a model  $f_{\tau,n}$  is obtained by applying an algorithm  $A_\tau$  to a training set  $S_{\tau,n}$  which consists of  $n$  samples drawn from a training distribution  $P_{\text{train}}$ .

$$f_{\tau,n} = A_\tau(S_{\tau,n}), \quad \text{where } S_{\tau,n} \sim P_{\text{train}}^n$$

**Generalization Factor.** To assess the model’s performance, we measure its effectiveness on both in-distribution (ID) and out-of-distribution (OOD) data.

- ID Performance: The ID performance,  $\Psi_{\text{ID}}^\tau(n)$ , is evaluated on a hold-out set from the same distribution  $P_{\text{train}}$

$$\Psi_{\text{ID}}^\tau(n) = \psi(f_{\tau,n}, P_{\text{train}})$$

- OOD Performance: The OOD performance,  $\Psi_{\text{OOD}}^\tau(n)$ , is the weighted average performance across a set of  $m$  distinct OOD distributions,  $Q = \{Q_1, \dots, Q_m\}$ , with weights defined by a distribution  $\alpha$ .

$$\Psi_{\text{OOD}}^\tau(n) = \mathbb{E}_{Q \sim \alpha} [\psi(f_{\tau,n}, Q)]$$

We establish a baseline model,  $f_{\tau,0}$ , which serves as a reference point. This is typically a pre-trained model that has not been fine-tuned on data of type  $\tau$ . The performance gains over this baseline are calculated as:

$$\begin{aligned} G_{\text{ID}}^\tau(n) &= \Psi_{\text{ID}}^\tau(n) - \Psi_{\text{ID}}^\tau(0) \\ G_{\text{OOD}}^\tau(n) &= \Psi_{\text{OOD}}^\tau(n) - \Psi_{\text{OOD}}^\tau(0) \end{aligned}$$

With a fixed number of samples  $n$ , we formalize the GF for data type  $\tau$ , denoted as  $\Gamma_\tau(n)$ , weighted harmonic mean of OOD performance gain and ID performance gain.

$$\Gamma_\tau(n) = \frac{(1 + \beta^2)G_{\text{OOD}}^\tau(n)G_{\text{ID}}^\tau(n)}{\beta^2G_{\text{ID}}^\tau(n) + G_{\text{OOD}}^\tau(n)}$$

where the weighting coefficient  $\beta$  is generally set to 2 to reflect the importance of the OOD performance gain in the generalization capabilities of the model. To ensure that the metric behaves well and is dimensionless, the evaluation function  $\psi$  should be normalized to a consistent range.

### 2.2 EXPERIMENTAL FINDINGS

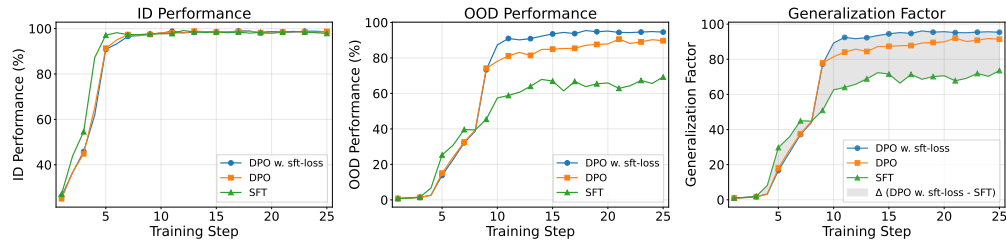


Figure 1: Performance Comparison: DPO vs. SFT on In-Distribution and Out-of-Distribution Task

To preliminarily examine how preference data and supervised data affect model generalization, we construct a preference dataset  $\mathcal{D}_{\text{pref}} = \{(x_i, y_i^+, y_i^-)\}_{i=1}^N$ , where  $y_i^+$  is the chosen response and  $y_i^-$  is the rejected response, and a supervised dataset  $\mathcal{D}_{\text{SFT}} = \{(x_i, y_i)\}_{i=1}^N$  with  $y_i = y_i^+$  around reasoning tasks defined by a specific answer format. Under equal data budgets, we evaluate two

settings: (i) an in-distribution setting in which the required reasoning format matches that used in training, and (ii) an out-of-distribution setting in which the required reasoning format differs<sup>2</sup>. We compare DPO training, SFT training, and DPO training augmented with SFT loss (see Section 3.3). The resulting  $G_{ID}^{\tau}(n)$ ,  $G_{OOD}^{\tau}(n)$ , and the  $\Gamma_{\tau}(n)$  are reported in Figure 1.

From the experimental results, it can be observed that SFT achieves the fastest convergence on ID tasks. However, due to its reliance on a single cross-entropy loss that maximizes the log-likelihood of the correct answer, it demonstrates poor OOD performance. By contrast, DPO converges more slowly at the beginning of ID tasks but yields better OOD performance. Remarkably, the model trained with a combination of DPO with SFT loss achieves the strongest generalization capability overall. As the number of training steps increases, the GF gap between the SFT training method and the DPO training method also increases.

### 3 METHODOLOGY: THE SPECS FRAMEWORK

#### 3.1 SELF-DISTILLED PREFERENCE COLD-START

A model with superior generalization capabilities provides a more effective starting point for RL. Inspired by the discussion in Section 2, we employ self-distillation to construct preference data focusing format learning. This data is then used in place of standard SFT data to enhance the model’s generalization performance during the cold-start phase.

To implement this, we propose SPECS, illustrated in Figure 2, a three-stage training optimization strategy consisting of 1) Self-Distillation for Preference Data Generation, 2) DPO-based Pre-Alignment for Cold-Start, and 3) Final GRPO Fine-tuning.

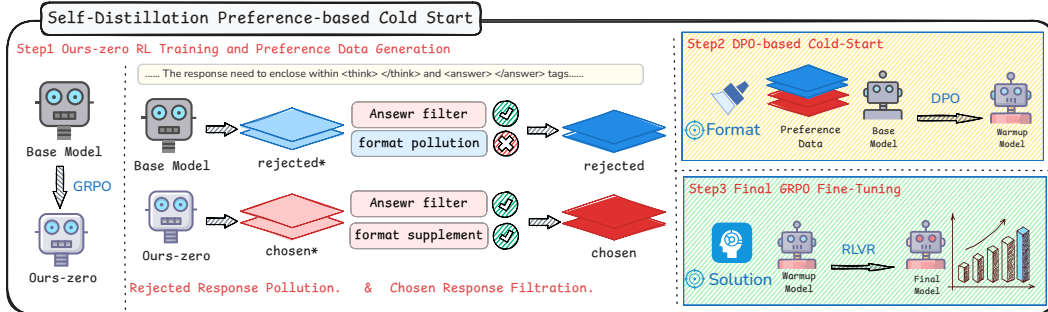


Figure 2: **Method Overview.** We propose the SPECS cold-start strategy, a three-stage pipeline to enhance final RL fine-tuning. Firstly, where we generate a preference dataset focused on teaching the correct output format by self distillation. Next, The base model is pre-aligned on this data using DPO to create a format-aware “Warmup Model”. Finally, this pre-aligned model undergoes Final RL tuning with GRPO, allowing the optimization process to focus on enhancing reasoning.

#### 3.2 SELF-DISTILLATION FOR PREFERENCE DATA GENERATION

**Objective:** The foundational stage of our framework aims to achieve two interconnected goals: first, to cultivate a preliminary “seed model” with enhanced reasoning capabilities, and second, to leverage this model to autonomously generate a high-quality preference dataset through a process we term self-distillation.

**Methodology:** A critical initial challenge is that a standard base VLM often lacks the capability to generate outputs of sufficient reasoning ability. To address this, we first conduct a brief, initial phase of RL fine-tuning on the base model using GRPO. This step aims not at achieving the final performance, but at creating an initial policy, denoted  $\pi_{GRPO-zero}$ , which is more adept at exploring the solution space.

<sup>2</sup>For more detailed description, see Appendix A.2

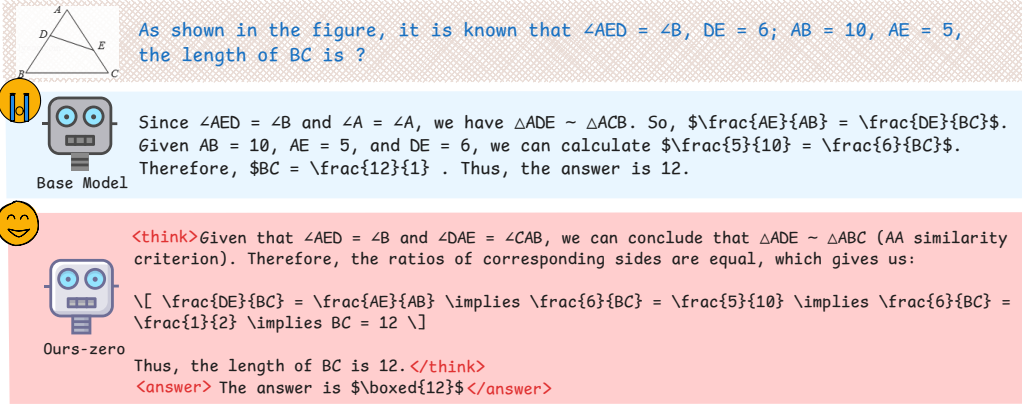


Figure 3: Example of a self-distilled preference data pair.

With the exploratory  $\pi_{GRPO-zero}$  model, we proceed to generate the preference dataset. The data construction process involves four key steps:

- **Response Generation.** We prompt two models, our exploratory  $\pi_{GRPO-zero}$  and  $\pi_{base}$ , with specific format instructions ( $<\text{think}>...</\text{think}><\text{answer}>...</\text{answer}>$ ) to create a dataset, which is designed to contain pairs of responses that are both correct in their final answer, but differ in their reasoning paradigm and answer format.
- **Chosen Response Filtration.** For the chosen response ( $y_i^+$ ), we use Gemini-2.5 flash (Comanici et al., 2025) as an evaluator. Assesses whether the reasoning path in the  $\pi_{GRPO-zero}$  response aligns correctly with its final answer. Only responses in which the reasoning and the answer are consistent are retained, forming a high-quality pool of candidates.
- **Rejected Response Pollution.** For the rejected response ( $y_i^-$ ), we select responses that also contain the correct answer, but deviate from the required format. Recognizing that some generated responses might incidentally have the correct format, We randomly apply one of the following five types of format corruption to these responses to ensure a clear learning signal.
  1. Remove all tags ( $<\text{think}>, </\text{think}>, <\text{answer}>, </\text{answer}>$ ).
  2. Remove the  $<\text{answer}>$  and  $</\text{answer}>$  tags.
  3. Remove the  $<\text{think}>$  and  $</\text{think}>$  tags.
  4. Remove the  $<\text{answer}>$  and  $</\text{answer}>$  tags and move the closing  $</\text{think}>$  tag to the end of the response.
  5. Replace the  $<\text{answer}>$  tags with the string `Answer:` and remove  $</\text{answer}>$  tags.
- **Preference Pair Construction via Self-Distillation.** We construct the chosen response and the rejected response into pairs of self-distilled preference data ( $y_i^+, y_i^-$ ). As shown in Figure 3. Both Chosen Responses ( $y_i^+$ ) and Rejected Responses ( $y_i^-$ ) are selected from the filtered pool and contain the correct final answer. This data set is designed to facilitate decoupled learning, separating the learning of reasoning paradigms and answer formats from the core logical reasoning ability. This approach serves as a more effective cold-start method for the final alignment stage.

### 3.3 DPO-BASED PRE-ALIGNMENT FOR COLD-START

**Objective:** The primary goal of this stage is to leverage the self-distilled preference dataset generated in the Stage 1 (Section 3.2) to pre-align the base VLM. This process yields a “cold-start” model that serves as a significantly improved starting point for the final reinforcement learning fine-tuning. We conceptualize this phase as a “warm-up,” which shifts the model’s policy into a more advantageous region of the policy landscape before the intensive final training.

**Methodology:** To achieve this pre-alignment, we employ DPO (Rafailov et al., 2023), a powerful technique that directly optimizes the language model on preference data without the need for an

explicit reward model. The standard DPO loss function is defined as:

$$\mathcal{L}_{DPO}(\pi_\theta; \pi_{ref}) = -\mathbb{E}_{(x, y_w, y_l) \sim D} \left[ \log \sigma \left( \beta \log \frac{\pi_\theta(y_w|x)}{\pi_{ref}(y_w|x)} - \beta \log \frac{\pi_\theta(y_l|x)}{\pi_{ref}(y_l|x)} \right) \right]$$

where  $\pi_\theta$  is the policy being optimized,  $\pi_{ref}$  is the reference policy (the initial base model),  $\beta$  is a temperature parameter, and  $(x, y_w, y_l)$  represents a triplet of prompt, chosen response, and rejected response from our self-distilled dataset D.

To augment this process, we incorporate an SFT loss computed on the “chosen” samples, which serves as a form of regularization. It ensures that while the model learns the directional preference signal from DPO, it does not drift far from the core distribution of high-quality text embodied by the chosen responses (Rao et al., 2025). The combined loss function is thus:

$$\mathcal{L}_{hybrid} = \mathcal{L}_{DPO} + \lambda \mathcal{L}_{SFT}$$

where  $\mathcal{L}_{SFT}$  is the conventional negative log-likelihood loss on the chosen responses, and  $\lambda$  is a weighting coefficient to balance the two objectives. For a discussion for  $\lambda$ , see Appendix A.3.

### 3.4 FINAL GRPO FINE-TUNING

**Objective:** To achieve peak performance by fine-tuning the pre-aligned cold-start model, focusing computational resources on enhancing complex reasoning capabilities.

**Methodology:** This final stage leverages the cold-start model obtained from Stage 2 as the initialization point for reinforcement learning, rather than starting from the base model or a conventional SFT model. The pre-alignment from the DPO phase ensures that the model has already mastered the output format. Consequently, the model is not required to expend resources on learning basic structural compliance. Instead, credit assignment during RL training can be more accurately attributed to the core challenge: improving the quality and precision of its reasoning process. This targeted optimization explains the observed stable convergence in our experiments and the model’s ability to achieve a higher performance ceiling.

For the final stage of fine-tuning, we employ the GRPO algorithm (Shao et al., 2024). This process is guided by a composite reward function that combines format and accuracy components to evaluate the model’s output,  $o$ , for a given question,  $q$ .

The total reward  $R_{total}$ , is the sum of a format reward  $R_{format}$ , and an accuracy reward  $R_{acc}$ :

$$R_{total}(o, q) = R_{format}(o) + R_{acc}(o, q)$$

**The format reward  $R_{format}(o)$** , assigns a fixed value of 0.5 for structurally correct outputs, reinforcing the policy’s formatting discipline.

**The accuracy reward  $R_{acc}(o, q)$** , provides a binary signal: 1.0 for a correct answer and 0 otherwise. We use a hybrid mechanism to determine correctness based on the question type,  $T(q)$ :

$$R_{acc}(o, q) = \begin{cases} R_{rule}(o, q) & \text{if } T(q) \in \{\text{Multiple-Choice, Numerical}\} \\ R_{lm}(o, q) & \text{if } T(q) = \text{Short-Answer} \end{cases}$$

For objective types like multiple-choice and numerical questions, a rule-based function assesses correctness. For subjective short-answer questions, we employ GPT-4o as an external judge.

## 4 EXPERIMENTS

### 4.1 EXPERIMENT SETTINGS

**Dataset and Benchmark:** The data utilized for training  $\pi_{GRPO-zero}$  model in Stage 1 and for the final GRPO fine-tuning of the cold-started model in Stage 3 is composed of the Orsta47K (Ma et al., 2025) and virl39K (Wang et al., 2025a) datasets. In Stage 2 of cold start training, we used 9K self-distilled data. This composition is designed to enhance the model’s general and mathematical

Table 1: Model performance comparison on MEGA-Bench Core.

Model	MEGA-Bench								MEGA-Bench Core
	Knowledge	Mathematics	Perception	Coding	Info. Ex.	Planning	Science	Metrics	
<i>Open-Source General Models</i>									
QwenVL-2-7B	39.96	25.95	39.99	31.49	40.29	16.64	28.59	43.61	34.47
QwenVL-2.5-7B	38.84	27.67	41.24	28.93	50.23	16.32	36.75	41.64	35.07
InternVL2-8B	33.94	22.08	32.15	24.7	29.13	12.17	24.61	39.96	25.96
InternVL2.5-8B	34.78	25.86	33.27	25.45	35.10	15.97	28.83	44.96	28.34
InternVL3-8B	<b>42.76</b>	<b>34.85</b>	42.76	<u>34.05</u>	44.84	17.10	35.21	<u>49.60</u>	36.02
Llava-OV-7B	31.37	22.11	27.64	13.9	17.07	9.16	24.38	37.31	21.36
Kimi-VL-A3B	37.63	27.07	39.50	22.30	40.99	<b>22.17</b>	33.94	46.65	34.40
<i>Open-Source Reasoning Models</i>									
R1-Onevision <sup>†</sup>	29.47	20.94	28.65	23.38	43.04	12.67	26.84	42.19	27.18
VLAA-Thinking <sup>†</sup>	38.23	28.83	40.73	28.84	44.58	17.05	36.69	45.57	34.86
Kimi-VL-A3B-Thinking	33.45	17.76	28.11	14.69	41.14	12.64	28.60	43.97	27.08
MM-Eureka-7B	40.12	31.59	39.71	28.75	49.32	16.64	<u>37.25</u>	46.39	35.96
VL-Rethinker-7B	40.65	30.08	42.02	29.87	<u>52.03</u>	17.83	36.82	46.90	37.25
Orsta-7B	41.65	31.48	<u>43.84</u>	32.82	<b>54.07</b>	17.83	36.91	41.66	<u>38.31</u>
Ours-zero	42.44	29.87	43.77	32.80	49.59	17.76	37.39	47.32	37.96
<b>Ours-7B</b>	<b>42.64</b>	<u>31.71</u>	<b>44.58</b>	<b>34.14</b>	51.68	<u>18.76</u>	<b>38.73</b>	<b>51.87</b>	<b>39.17</b>
Δ (Ours - Backbone)	+3.8	+4.0	+3.3	+5.2	+1.4	+2.4	+2.0	+10.2	+4.1

<sup>1</sup> The †symbol indicates that the results were evaluated with VLMEvalKit<sup>3</sup>.<sup>2</sup> The remaining results are from the MEGA-Bench Leaderboard and Ma et al. (2025).

Table 2: Model Performance Comparison On Other Benchmarks

Model	MMMU val	MathVision	MathVisita	MathVerse vision only	Overall
<i>Backbone</i>					
QwenVL-2.5-7B	54.2†	25.40	63.70	38.20	45.38
<i>QwenVL-2.5-7B based Reasoning Models</i>					
R1-Onevision	49.67†	<b>29.90</b>	64.1	40.0	45.92
VLAA-Thinking	52.67†	26.40	68.00	48.20	48.82
MM-Eureka-7B	55.55†	26.90	73.00	47.58†	50.76
VL-Rethinker-7B	56.7	<u>29.70</u>	<u>73.60</u>	<b>48.98†</b>	<u>52.25</u>
Orsta-7B†	54.33	25.76	70.20	32.10	45.60
Ours-zero	54.3	26.88	72.90	47.33	50.35
<b>Ours-7B</b>	<b>56.78</b>	29.50	<b>75.90</b>	<u>48.73</u>	<b>52.73</b>
Δ (Ours - Backbone)	+2.5	+4.1	+12.2	+10.5	+7.3

The †symbol indicates that the results were evaluated with VLMEvalKit<sup>4</sup>.

reasoning capabilities. We conduct evaluations on multiple benchmark datasets, including MEGA-Bench (Chen et al., 2025b), MMMU (Yue et al., 2024), MathVista (Lu et al., 2024b), MATH-Vision (Wang et al., 2024a), and MathVerse (Zhang et al., 2024).

**Baseline:** Our comparative analysis is grounded on two primary categories of models. The first category comprises open-source general VLMs, including QwenVL-2-7B (Wang et al., 2024b), QwenVL-2.5-7B (Bai et al., 2025), InternVL2-8B (Chen et al., 2024), InternVL2.5-8B (Chen et al., 2024), Kimi-VL-A3B (Team et al., 2025), and DeepSeek-VL-7B (Lu et al., 2024a). The second category focuses on models specifically engineered for advanced reasoning tasks. This group includes Kimi-VL-A3B-Thinking (Team et al., 2025), R1-Onevision (Yang et al., 2025), VLAA-Thinking (Chen et al., 2025a), MM-Eureka-7B (Meng et al., 2025), VL-Rethinker-7B (Wang et al., 2025a), and Orsta-7B (Ma et al., 2025).

**Implementation Details:** We utilize the open-source Multimodal Large Language Model, Qwen2.5-VL-7B (Bai et al., 2025), as our base model. For the GRPO training in Stage 1 and Stage 3, we employ the MM-EUREKA<sup>5</sup> framework. The rollout and training batch sizes are both set to 128, with 8 rollouts generated per sample. The learning rate is configured to  $1 \times 10^{-6}$ . For the DPO training in Stage 2, as well as for the comparative SFT experiments, we leverage the LlamaFactory<sup>6</sup> framework. In this configuration, the training batch size is set to 64, the learning rate is maintained

<sup>5</sup><https://github.com/ModalMinds/MM-EUREKA><sup>6</sup><https://github.com/hiouga/LLaMA-Factory>

at  $1 \times 10^{-6}$ , and the hyperparameter  $\lambda$  for the hybrid loss function is set to 1. The prompt used during training is shown in Appendix A.2.

## 4.2 MAIN RESULTS

Table 1 presents the overall performance of our model on MEGA-Bench Core, along with the scores for each subtask, in comparison with other baseline models. Table 2 reports the performance of various inference models built on the QwenVL-2.5-7B backbone across additional benchmarks. Our model has improvements in general task benchmarks (MEGA-BENCH core, MMMU) and mathematical reasoning benchmarks (MathVision, MathVisita, MathVerse), and some benchmarks are in a leading position among models of the same size, demonstrating the effectiveness of our approach.

## 4.3 ABLATION ON SELF-DISTILLATION AND DECOUPLED DATA STRATEGY

**Self-distillation proves more effective than external teacher models.** First, we evaluate the effectiveness of the self-distillation mechanism by substituting it with preference data generated from powerful external teacher models, specifically QwenVL-2.5-32B and QwenVL-2.5-72B. The results shown in Tabel 3 clearly indicate that our self-distillation approach outperforms both teacher-based alternatives. We also observe that performance degradation is more pronounced when using the QwenVL-2.5-32B model, whose output distribution diverges more significantly from our base model. This finding suggests that preference data closely aligned with the model’s intrinsic capability distribution is more effective for alignment than guidance from a more capable but dissimilar external model.

**The decoupled data strategy outperforms the coupled approach for DPO cold-starting.** Next, we investigate the impact of our decoupled data strategy for DPO cold-starting. We compare it against a “coupled” DPO approach, where preference data is mixed, containing pairs that differ in both answer correctness and reasoning format. In contrast, our decoupled strategy strictly uses preference pairs where both chosen and rejected responses feature correct answers but diverge in their reasoning format. The experimental results shown in Table 3 demonstrate the clear superiority of the decoupled approach.

Table 3: Ablation Results to show the impact of Self Distillation and Decoupled Data

Model	Megabench	MMMU	MathVista	MathVision	MathVerse	AVG
Qwen-VL-2.5-7B	35.07	54.2	63.70	25.40	38.20	43.31
- Qwen32b Distillation	27.04 / 29.87	51.44 / 56.67	66.90 / 71.50	25.53 / 28.03	43.53 / 46.07	42.89 / 46.43
- Qwen72b Distillation	34.00 / 37.30	53.89 / 58.56	67.50 / 73.30	25.62 / 28.91	43.53 / 46.83	44.90 / 48.98
- <i>Self Distillation</i>	37.52 / 39.17	54.89 / 56.78	72.00 / 75.90	25.75 / 29.50	46.19 / 48.73	47.27 / 50.02
- Coupled Data	37.02 / 38.76	55.44 / 55.44	71.10 / 73.10	27.37 / 28.65	47.46 / 47.46	47.67 / 48.68
- <i>Decoupled Data</i>	37.52 / 39.17	54.89 / 56.78	72.00 / 75.90	25.75 / 29.50	46.19 / 48.73	47.27 / 50.02

The value on the left side of the slash ‘/’ represents the score after cold-start training, and the value on the right side of the slash represents the score after cold start + RL.

## 4.4 ANALYSIS OF THE RELATIONSHIP BETWEEN GF AND FINAL PERFORMANCE

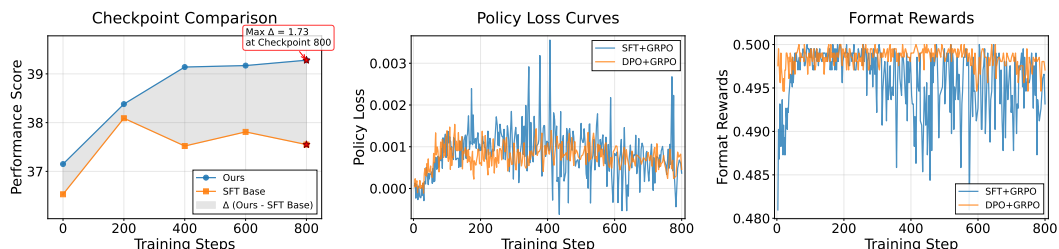


Figure 4: Impact on RL Training Efficiency and stability.

We evaluate the correlation between the model’s GF value during the cold-start phase and its final performance (represented here by the average score on MEGA-Bench, MMMU, and MathVerse\_Vision\_Only). By comparing three cold-start methods with different GF values, presented in Figure 5, we can see that GF and the model’s final performance are correlated to a certain extent. This also confirms that the stronger the model’s generalization ability in the cold-start phase, the more it will contribute to the model’s improvement in the RL phase.

In addition, we can also prove that the cold-start method based on preference data has higher generalization ability compared with the traditional SFT cold-start paradigm, thus bringing greater potential for improvement to subsequent RL.

#### 4.5 ANALYSIS OF THE IMPACT ON RL TRAINING EFFICIENCY AND STABILITY

We examine the downstream effects of our DPO cold-start strategy, assessing its impact on the efficiency and stability of the final RL phase.

**Performance and Training Efficiency.** To evaluate performance and training efficiency, we tracked MEGA-Bench scores throughout the GRPO training process. As illustrated in Figure 4, the DPO+GRPO model begins with a substantially higher initial score, demonstrating the immediate benefit of preference-based pre-alignment. Furthermore, it maintains a clear advantage throughout training, converging more rapidly and ultimately achieving a higher performance ceiling than its SFT+GRPO counterpart. For more analysis on this content, please refer to Appendix A.3.

**Training Stability.** Beyond performance metrics, we analyzed training stability by comparing the policy loss curves, presented in Figure 4. The curve for DPO+GRPO is visibly smoother and more stable, indicating a more consistent and reliable optimization trajectory. In contrast, the SFT+GRPO policy exhibits greater volatility, suggesting that the RL algorithm must make more drastic and potentially erratic updates. In terms of format rewards, RL based on SFT cold start is also weaker than RL based on DPO cold start in terms of the stability of format rewards.

## 5 RELATED WORK

For a more detailed introduction to related work, please refer to Appendix A.5.

**RL for Multimodal Reasoning.** The application of RL has proven to be a highly effective method for enhancing the reasoning capabilities of large language models, with notable successes such as DeepSeek-R1 (Guo et al., 2025) which leverages RLVR (Lambert et al., 2024; Guo et al., 2025). Inspired by these advancements in the text-only domain, a substantial and rapidly growing body of research has begun to adapt these RL techniques for VLMs. This has catalyzed a wave of “MLM-r1” studies (Meng et al., 2025; Shen et al., 2025; Peng et al., 2025; Zhou et al., 2025; Zhang et al., 2025a; Wang et al., 2025b;a; Zheng et al., 2025; Ma et al., 2025), all aiming to harness similar principles to unlock more advanced multimodal reasoning abilities.

**Cold-Start Strategies and Data Generation.** A crucial precursor to effective reinforcement learning is the “cold-start” phase, which initializes the model policy. The predominant strategy for this phase is SFT on high-quality instruction-response pairs (Wei et al., 2025; Yang et al., 2025; Huang et al., 2025; Deng et al., 2025b). In parallel, the prohibitive cost of human annotation has driven the field towards synthetic data generation, often using powerful teacher models to distill data for smaller student models (Zhang et al., 2025b; Yao et al., 2024; Xu et al., 2024; Huang et al., 2025).

## 6 CONCLUSIONS

In this study, we introduced the Self-Distilled Preference-based Cold-Start framework, a novel three-stage methodology. By leveraging a self-distillation process to generate preference data, we decouple the learning of shallow objectives, such as output format, from the deep, logical reasoning skills targeted during the final RL phase. Our method utilizes DPO to pre-align the model, providing a superior initial policy for RL. The creative insight of decoupling learning objectives solves the practical problem of SFT-induced overfitting, which often constrains exploration and leads to sub-optimal performance. Our results demonstrate the practical value of this approach. The introduction of the Generalization Factor also provides a valuable new metric for quantifying model generalization. This work shows considerable application prospects for developing more robust and capable multimodal reasoning systems.

Despite these promising results, this study has certain limitations that suggest avenues for future research. Our experiments were focused on the multimodal domain; further studies should be conducted to validate the efficacy of the SPECS framework in text-only reasoning tasks. The generalization of our findings could also be strengthened through more extensive testing across a more diverse set of out-of-distribution benchmarks. Such investigations would continue to refine our understanding of how to most effectively structure learning pipelines for complex AI systems.

### ETHICS STATEMENT

All of the paper’s authors have read and adhered to the ICLR Code of Ethics. This work focuses on advancing the reasoning capabilities of multimodal large language models through a novel training methodology. The core contributions are algorithmic, aimed at improving the efficiency, stability, and performance ceiling of reinforcement learning pipelines for such models.

**Data and Models:** The datasets used for training and evaluation, including Orsta47K, virl39K, MEGA-Bench, MMMU, MathVista, MATH-Vision, and MathVerse, are publicly available datasets and benchmarks established within the academic community. Our use of these standard datasets is intended to ensure transparency, facilitate reproducibility, and allow for direct comparison with prior work. We do not use any private or sensitive user data. The base model used, Qwen2.5-VL-7B, is an open-source model, promoting accessibility and further research.

**External Evaluators:** For evaluating subjective short-answer questions where automated rule-based metrics are insufficient, we employed proprietary models (GPT-4o) as external judges. We acknowledge that these models may have their own inherent biases. This approach was chosen to provide a consistent and scalable evaluation standard for complex, open-ended responses, a common practice in current AI research. The specific prompts and evaluation criteria were designed to be as objective as possible to mitigate these potential biases.

**Potential Societal Impact:** The goal of this research is to enhance the general reasoning abilities of AI systems. While this can lead to positive applications in fields like education, scientific research, and accessibility tools, we recognize that, like any powerful technology, it could potentially be misused. Our work does not introduce any new applications but rather improves the underlying training methodology. We encourage the responsible development and deployment of AI systems built upon these foundational research advancements.

**Bias and Fairness:** Our proposed framework, SPECS, is not designed for a specific downstream application and was evaluated on broad-domain academic benchmarks. We have not conducted an in-depth analysis of social or demographic biases, as the datasets primarily consist of math, science, and general knowledge problems. We acknowledge that the underlying base model and training data may contain biases, and future work should investigate how different training strategies impact the propagation or mitigation of such biases.

### REPRODUCIBILITY STATEMENT

To ensure the reproducibility of our work, we provide a detailed account of our methodology and experimental setup. The core SPECS framework, including its three stages of self-distillation for data generation, DPO-based pre-alignment, and final GRPO fine-tuning, is described in Section 3. Our complete experimental settings, including the datasets, benchmarks, and baselines used for eval-

ation, are detailed in Section 4.1 . This section also specifies crucial implementation details, such as learning rates and batch sizes for all training stages . We utilized publicly available frameworks, MM-EUREKA and LlamaFactory, for our implementation. Furthermore, the appendix offers additional resources to aid in reproduction, including the exact system prompts used for training and inference (Appendix A.2) and a detailed analysis of the hybrid loss coefficient (Appendix A.3).

## REFERENCES

- Shuai Bai, Keqin Chen, Xuejing Liu, Jialin Wang, Wenbin Ge, Sibo Song, Kai Dang, Peng Wang, Shijie Wang, Jun Tang, Humen Zhong, Yuanzhi Zhu, Mingkun Yang, Zhaohai Li, Jianqiang Wan, Pengfei Wang, Wei Ding, Zheren Fu, Yiheng Xu, Jiabo Ye, Xi Zhang, Tianbao Xie, Zesen Cheng, Hang Zhang, Zhibo Yang, Haiyang Xu, and Junyang Lin. Qwen2.5-vl technical report. *arXiv preprint arXiv:2502.13923*, 2025.
- Yoshua Bengio, Jérôme Louradour, Ronan Collobert, and Jason Weston. Curriculum learning. In *Proceedings of the 26th annual international conference on machine learning*, pp. 41–48, 2009.
- Hardy Chen, Haoqin Tu, Fali Wang, Hui Liu, Xianfeng Tang, Xinya Du, Yuyin Zhou, and Cihang Xie. Sft or rl? an early investigation into training rl-like reasoning large vision-language models. *arXiv preprint arXiv:2504.11468*, 2025a.
- Jiacheng Chen, Tianhao Liang, Sherman Siu, Zhengqing Wang, Kai Wang, Yubo Wang, Yuansheng Ni, Wang Zhu, Ziyan Jiang, Bohan Lyu, Dongfu Jiang, Xuan He, Yuan Liu, Hexiang Hu, Xiang Yue, and Wenhui Chen. Mega-bench: Scaling multimodal evaluation to over 500 real-world tasks. In *International Conference on Learning Representations (ICLR)*, 2025b.
- Zhe Chen, Jiannan Wu, Wenhui Wang, Weijie Su, Guo Chen, Sen Xing, Muyan Zhong, Qinglong Zhang, Xizhou Zhu, Lewei Lu, et al. Internvl: Scaling up vision foundation models and aligning for generic visual-linguistic tasks. In *Proceedings of the IEEE/CVF Conference on Computer Vision and Pattern Recognition*, pp. 24185–24198, 2024.
- Tianzhe Chu, Yuexiang Zhai, Jihan Yang, Shengbang Tong, Saining Xie, Dale Schuurmans, Quoc V Le, Sergey Levine, and Yi Ma. Sft memorizes, rl generalizes: A comparative study of foundation model post-training. *arXiv preprint arXiv:2501.17161*, 2025.
- Gheorghe Comanici, Eric Bieber, Mike Schaeckermann, Ice Pasupat, Noveen Sachdeva, Inderjit Dhillon, Marcel Blistein, Ori Ram, Dan Zhang, Evan Rosen, et al. Gemini 2.5: Pushing the frontier with advanced reasoning, multimodality, long context, and next generation agentic capabilities. *arXiv preprint arXiv:2507.06261*, 2025.
- Jia Deng, Jie Chen, Zhipeng Chen, Daixuan Cheng, Fei Bai, Beichen Zhang, Yinqian Min, Yanzipeng Gao, Wayne Xin Zhao, and Ji-Rong Wen. From trial-and-error to improvement: A systematic analysis of llm exploration mechanisms in rlvr. *arXiv preprint arXiv:2508.07534*, 2025a.
- Yihe Deng, Hritik Bansal, Fan Yin, Nanyun Peng, Wei Wang, and Kai-Wei Chang. Openvlthinker: An early exploration to complex vision-language reasoning via iterative self-improvement. *arXiv preprint arXiv:2503.17352*, 2025b.
- Daya Guo, Dejian Yang, Haowei Zhang, Junxiao Song, Ruoyu Zhang, Runxin Xu, Qihao Zhu, Shirong Ma, Peiyi Wang, Xiao Bi, et al. Deepseek-rl: Incentivizing reasoning capability in llms via reinforcement learning. *arXiv preprint arXiv:2501.12948*, 2025.
- Wenxuan Huang, Bohan Jia, Zijie Zhai, Shaosheng Cao, Zheyu Ye, Fei Zhao, Zhe Xu, Yao Hu, and Shaohui Lin. Vision-rl: Incentivizing reasoning capability in multimodal large language models. *arXiv preprint arXiv:2503.06749*, 2025.
- Nathan Lambert, Jacob Morrison, Valentina Pyatkin, Shengyi Huang, Hamish Ivison, Faeze Brahman, Lester James V Miranda, Alisa Liu, Nouha Dziri, Shane Lyu, et al. Tulu 3: Pushing frontiers in open language model post-training. *arXiv preprint arXiv:2411.15124*, 2024.

Haoyu Lu, Wen Liu, Bo Zhang, Bingxuan Wang, Kai Dong, Bo Liu, Jingxiang Sun, Tongzheng Ren, Zhuoshu Li, Yaofeng Sun, Chengqi Deng, Hanwei Xu, Zhenda Xie, and Chong Ruan. Deepseek-vl: Towards real-world vision-language understanding, 2024a.

Pan Lu, Hritik Bansal, Tony Xia, Jiacheng Liu, Chunyuan Li, Hannaneh Hajishirzi, Hao Cheng, Kai-Wei Chang, Michel Galley, and Jianfeng Gao. Mathvista: Evaluating mathematical reasoning of foundation models in visual contexts. In *International Conference on Learning Representations (ICLR)*, 2024b.

Yan Ma, Linge Du, Xuyang Shen, Shaoxiang Chen, Pengfei Li, Qibing Ren, Lizhuang Ma, Yuchao Dai, Pengfei Liu, and Junjie Yan. One rl to see them all: Visual triple unified reinforcement learning. *arXiv preprint arXiv:2505.18129*, 2025.

Fanqing Meng, Lingxiao Du, Zongkai Liu, Zhixiang Zhou, Quanfeng Lu, Daocheng Fu, Tiancheng Han, Botian Shi, Wenhui Wang, Junjun He, Kaipeng Zhang, Ping Luo, Yu Qiao, Qiaosheng Zhang, and Wenqi Shao. Mm-eureka: Exploring the frontiers of multimodal reasoning with rule-based reinforcement learning. *arXiv preprint arXiv:2503.07365*, 2025.

Yingzhe Peng, Gongrui Zhang, Miaosen Zhang, Zhiyuan You, Jie Liu, Qipeng Zhu, Kai Yang, Xingzhong Xu, Xin Geng, and Xu Yang. Lmm-r1: Empowering 3b lmms with strong reasoning abilities through two-stage rule-based rl. *arXiv preprint arXiv:2503.07536*, 2025.

Rafael Rafailov, Archit Sharma, Eric Mitchell, Christopher D Manning, Stefano Ermon, and Chelsea Finn. Direct preference optimization: Your language model is secretly a reward model. *Advances in neural information processing systems*, 36:53728–53741, 2023.

Jun Rao, Zepeng Lin, Xuebo Liu, Xiaopeng Ke, Lian Lian, Dong Jin, Shengjun Cheng, Jun Yu, and Min Zhang. Apt: Improving specialist llm performance with weakness case acquisition and iterative preference training. *arXiv preprint arXiv:2506.03483*, 2025.

Zhihong Shao, Peiyi Wang, Qihao Zhu, Runxin Xu, Junxiao Song, Xiao Bi, Haowei Zhang, Mingchuan Zhang, YK Li, Yang Wu, et al. Deepseekmath: Pushing the limits of mathematical reasoning in open language models. *arXiv preprint arXiv:2402.03300*, 2024.

Haozhan Shen, Peng Liu, Jingcheng Li, Chunxin Fang, Yibo Ma, Jiajia Liao, Qiaoli Shen, Zilun Zhang, Kangjia Zhao, Qianqian Zhang, Ruochen Xu, and Tiancheng Zhao. Vlm-r1: A stable and generalizable rl-style large vision-language model. *arXiv preprint arXiv:2504.07615*, 2025.

Kimi Team, Angang Du, Bohong Yin, Bowei Xing, Bowen Qu, Bowen Wang, Cheng Chen, Chenlin Zhang, Chenzhuang Du, Chu Wei, Congcong Wang, Dehao Zhang, Dikang Du, Dongliang Wang, Enming Yuan, Enzhe Lu, Fang Li, Flood Sung, Guangda Wei, Guokun Lai, Han Zhu, Hao Ding, Hao Hu, Hao Yang, Hao Zhang, Haoning Wu, Haotian Yao, Haoyu Lu, Heng Wang, Hongcheng Gao, Huabin Zheng, Jiaming Li, Jianlin Su, Jianzhou Wang, Jiaqi Deng, Jiezhong Qiu, Jin Xie, Jinhong Wang, Jingyuan Liu, Junjie Yan, Kun Ouyang, Liang Chen, Lin Sui, Longhui Yu, Mengfan Dong, Mengnan Dong, Nuo Xu, Pengyu Cheng, Qizheng Gu, Runjie Zhou, Shaowei Liu, Sihan Cao, Tao Yu, Tianhui Song, Tongtong Bai, Wei Song, Weiran He, Weixiao Huang, Weixin Xu, Xiaokun Yuan, Xingcheng Yao, Xingzhe Wu, Xinxing Zu, Xinyu Zhou, Xinyuan Wang, Y. Charles, Yan Zhong, Yang Li, Yangyang Hu, Yanru Chen, Yejie Wang, Yibo Liu, Yibo Miao, Yidao Qin, Yimin Chen, Yiping Bao, Yiqin Wang, Yongsheng Kang, Yuanxin Liu, Yulun Du, Yuxin Wu, Yuzhi Wang, Yuzi Yan, Zaida Zhou, Zhaowei Li, Zhejun Jiang, Zheng Zhang, Zhilin Yang, Zhiqi Huang, Zihao Huang, Zijia Zhao, and Ziwei Chen. Kimi-VL technical report, 2025. URL <https://arxiv.org/abs/2504.07491>.

Haozhe Wang, Chao Qu, Zuming Huang, Wei Chu, Fangzhen Lin, and Wenhui Chen. Vl-rethinker: Incentivizing self-reflection of vision-language models with reinforcement learning. *arXiv preprint arXiv:2504.08837*, 2025a.

Ke Wang, Junting Pan, Weikang Shi, Zimu Lu, Houxing Ren, Aojun Zhou, Mingjie Zhan, and Hongsheng Li. Measuring multimodal mathematical reasoning with math-vision dataset. In *The Thirty-eight Conference on Neural Information Processing Systems Datasets and Benchmarks Track*, 2024a. URL <https://openreview.net/forum?id=QWTCCxMpPA>.

- Peng Wang, Shuai Bai, Sinan Tan, Shijie Wang, Zhihao Fan, Jinze Bai, Keqin Chen, Xuejing Liu, Jialin Wang, Wenbin Ge, Yang Fan, Kai Dang, Mengfei Du, Xuancheng Ren, Rui Men, Dayiheng Liu, Chang Zhou, Jingren Zhou, and Junyang Lin. Qwen2-vl: Enhancing vision-language model's perception of the world at any resolution. *arXiv preprint arXiv:2409.12191*, 2024b.
- Xiyao Wang, Zhengyuan Yang, Chao Feng, Hongjin Lu, Linjie Li, Chung-Ching Lin, Kevin Lin, Furong Huang, and Lijuan Wang. Sota with less: Mcts-guided sample selection for data-efficient visual reasoning self-improvement. *arXiv preprint arXiv:2504.07934*, 2025b.
- Lai Wei, Yuting Li, Kaipeng Zheng, Chen Wang, Yue Wang, Linghe Kong, Lichao Sun, and Weiran Huang. Advancing multimodal reasoning via reinforcement learning with cold start. *arXiv preprint arXiv:2505.22334*, 2025.
- Yongliang Wu, Yizhou Zhou, Zhou Ziheng, Yingzhe Peng, Xinyu Ye, Xinting Hu, Wenbo Zhu, Lu Qi, Ming-Hsuan Yang, and Xu Yang. On the generalization of sft: A reinforcement learning perspective with reward rectification. *arXiv preprint arXiv:2508.05629*, 2025.
- Guowei Xu, Peng Jin, Ziang Wu, Hao Li, Yibing Song, Lichao Sun, and Li Yuan. Llava-cot: Let vision language models reason step-by-step. *arXiv preprint arXiv:2411.10440*, 2024.
- Yi Yang, Xiaoxuan He, Hongkun Pan, Xiyan Jiang, Yan Deng, Xingtao Yang, Haoyu Lu, Dacheng Yin, Fengyun Rao, Minfeng Zhu, et al. R1-onevision: Advancing generalized multimodal reasoning through cross-modal formalization. *arXiv preprint arXiv:2503.10615*, 2025.
- Huanjin Yao, Jiaxing Huang, Wenhao Wu, Jingyi Zhang, Yibo Wang, Shunyu Liu, Yingjie Wang, Yuxin Song, Haocheng Feng, Li Shen, et al. Mulberry: Empowering mllm with o1-like reasoning and reflection via collective monte carlo tree search. *arXiv preprint arXiv:2412.18319*, 2024.
- Xiang Yue, Yuansheng Ni, Kai Zhang, Tianyu Zheng, Ruoqi Liu, Ge Zhang, Samuel Stevens, Dongfu Jiang, Weiming Ren, Yuxuan Sun, et al. Mmmu: A massive multi-discipline multimodal understanding and reasoning benchmark for expert agi. In *Proceedings of the IEEE/CVF Conference on Computer Vision and Pattern Recognition*, pp. 9556–9567, 2024.
- Chen Zhang, Dawei Song, Zheyu Ye, and Yan Gao. Towards the law of capacity gap in distilling language models. *arXiv preprint arXiv:2311.07052*, 2023.
- Jingyi Zhang, Jiaxing Huang, Huanjin Yao, Shunyu Liu, Xikun Zhang, Shijian Lu, and Dacheng Tao. R1-vl: Learning to reason with multimodal large language models via step-wise group relative policy optimization. *arXiv preprint arXiv:2503.12937*, 2025a.
- Letian Zhang, Quan Cui, Bingchen Zhao, and Cheng Yang. Oasis: One image is all you need for multimodal instruction data synthesis. *arXiv preprint arXiv:2503.08741*, 2025b.
- Renrui Zhang, Dongzhi Jiang, Yichi Zhang, Haokun Lin, Ziyu Guo, Pengshuo Qiu, Aojun Zhou, Pan Lu, Kai-Wei Chang, Peng Gao, et al. Mathverse: Does your multi-modal llm truly see the diagrams in visual math problems? *arXiv preprint arXiv:2403.14624*, 2024.
- Ziwei Zheng, Michael Yang, Jack Hong, Chenxiao Zhao, Guohai Xu, Le Yang, Chao Shen, and Xing Yu. Deepeyes: Incentivizing” thinking with images” via reinforcement learning. *arXiv preprint arXiv:2505.14362*, 2025.
- Hengguang Zhou, Xirui Li, Ruochen Wang, Minhao Cheng, Tianyi Zhou, and Cho-Jui Hsieh. R1-zero’s” aha moment” in visual reasoning on a 2b non-sft model. *arXiv preprint arXiv:2503.05132*, 2025.

## A APPENDIX

### A.1 THE USE OF LARGE LANGUAGE MODELS

In preparing this manuscript, we utilized the Large Language Model (LLM) Gemini-2.5-pro (Comanici et al., 2025) to polishing the text. Its application was strictly limited to correcting spelling and grammatical errors. The authors manually reviewed and verified all AI-assisted modifications to ensure factual accuracy. The core ideas, methodologies, and figures presented are entirely the original work of the human authors.

### A.2 PROMPTS

The following are the System Prompts for the model during the cold start training phase and the RL training phase. In the instruction format generalization experiment in Section 2, the Inference System Prompt for the ID Task is consistent with these.

#### System Prompt for Cold Start Training and ID Task Inference

```
Solve the question. The user asks a question, and you solve it. You first think about the reasoning process in the mind and then provide the user with the answer. The answer is in latex format and wrapped in $...$. The final answer must be wrapped using the \boxed{} command. The reasoning process and answer are enclosed within <think> </think> and <answer> </answer> tags, respectively, i.e., <think> Since $1+1=2$, so the answer is $2$. </think> <answer> The answer is $\\boxed{2}$ </answer>, which means assistant's output should start with <think> and end with </answer>.
```

The following is the Inference System Prompt for the OOD Task in the instruction format generalization experiment of Section 2.

#### System Prompt for OOD Task Inference

```
Solve the question. The user asks a question, and you solve it. You first think about the reasoning process in the mind and then provide the user with the answer. The answer is in latex format and wrapped in $...$. The final answer must be wrapped using the \boxed{} command. The reasoning process and answer are enclosed within <cot> </cot> and <response> </response> tags, respectively, i.e., <cot> Since $1+1=2$, so the answer is $2$. </cot> <response> The answer is $\\boxed{2}$ </response>, which means assistant's output should start with <cot> and end with </response>.
```

### A.3 ANALYSIS OF LOSS BALANCE COEFFICIENTS IN COLD-START TRAINING

#### A.3.1 PRELIMINARIES

**Supervised Fine-Tuning.** SFT adapts pre-trained models by optimizing a cross-entropy loss function to maximize the log-likelihood of a desired output  $y_c$  for a given prompt  $x$ . The loss is defined as:

$$\mathcal{L}_{SFT}(\pi_\theta) = \mathbb{E}_{(x,y_c) \sim D} [-\log \pi_\theta(y_c|x)]$$

By training exclusively on positive examples, SFT creates a sharply peaked probability distribution that closely mimics the training data. While this accelerates model convergence, it can limit generalization capabilities.

**Direct Preference Optimization.** DPO(Rafailov et al., 2023) refines models by learning directly from preference data, consisting of a prompt  $x$ , a chosen response  $y_c$ , and a rejected response  $y_r$ .

The DPO loss function is designed to increase the relative probability of the chosen response over the rejected one:

$$\mathcal{L}_{DPO}(\pi_\theta; \pi_{\text{ref}}) = -\mathbb{E}_{(x, y_c, y_r) \sim D} \left[ \log \sigma \left( \beta \log \frac{\pi_\theta(y_c|x)}{\pi_{\text{ref}}(y_c|x)} - \beta \log \frac{\pi_\theta(y_r|x)}{\pi_{\text{ref}}(y_r|x)} \right) \right]$$

where  $\pi_\theta$  is the policy being optimized,  $\pi_{\text{ref}}$  is a reference policy,  $\sigma$  is the logistic function and  $\beta$  is a temperature parameter. This approach maximizes the margin between chosen and rejected responses, cultivating a smoother and more robust probability distribution that enhances the model’s generalization performance.

### A.3.2 ANALYSIS OF LOSS BALANCE COEFFICIENTS

In Section 3.3, we proposed that in our cold start, in addition to the basic DPO loss, we also added the SFT loss to ensure that the model does not deviate too much from the chosen samples during the training process. The combined loss function is thus:

$$\mathcal{L}_{\text{hybrid}} = \mathcal{L}_{DPO} + \lambda \mathcal{L}_{SFT}$$

Among the  $\mathcal{L}_{\text{hybrid}}$ , the DPO loss function is designed to increase the relative probability of the chosen response over the rejected one:

$$\mathcal{L}_{DPO}(\pi_\theta; \pi_{\text{ref}}) = -\mathbb{E}_{(x, y_c, y_r) \sim D} \left[ \log \sigma \left( \beta \log \frac{\pi_\theta(y_c|x)}{\pi_{\text{ref}}(y_c|x)} - \beta \log \frac{\pi_\theta(y_r|x)}{\pi_{\text{ref}}(y_r|x)} \right) \right]$$

We recorded the model’s rewards for chosen, rewards for rejected, and margins during cold start training when  $\lambda = 0$ ,  $\lambda = 0.5$ , and  $\lambda = 1$ , as shown in Figure 6 below.

From the picture, we can see a lot. Since the training loss of DPO can expand the margin between the chosen and the rejected, when  $\lambda = 0$ , this margin is the largest. However, this margin causes both the chosen and rejected rewards to decrease (the rejected rewards decrease faster than the chosen rewards). When  $\lambda = 0.5$  and  $\lambda = 1$ , it ensures that the chosen rewards increase during the DPO training process.

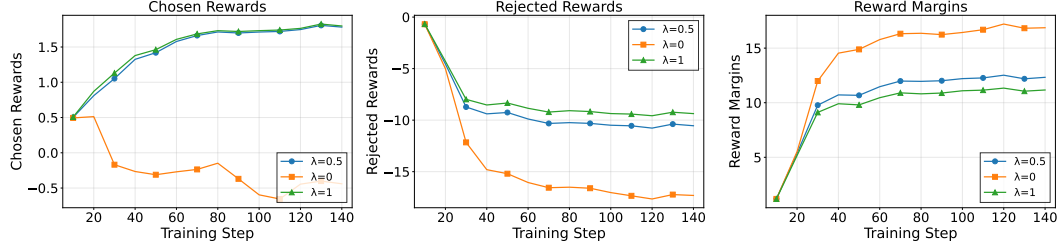


Figure 6: Effect of  $\lambda$  on Chosen and Rejected Rewards and Reward Margins During Training

### A.4 PERFORMANCE POTENTIAL OF DPO-BASED COLD-START VS. SFT

Table 4: Average RBF by Sample Size

Model \ Sample Size	120	240	480
base	1.7686	1.9166	1.9206
sft	1.8086	1.8961	1.9336
ours	<b>1.8216</b>	<b>1.9268</b>	<b>1.9596</b>

To evaluate the effectiveness of our proposed cold-start strategy, we first compare our DPO-based approach against a conventional SFT baseline. For this comparison, the SFT model was fine-tuned exclusively on the “chosen” responses from our preference dataset, while our model was trained using the full preference pairs with the DPO algorithm.

**Performance Potential via Pass@K.** We assessed the performance of both the DPO and SFT cold-start models on the MMMU benchmark. As delineated in Figure 7, the DPO-based model demonstrates superior performance across evaluated metrics, including Pass@8, and Pass@32. This indicates that the DPO cold-start method endows the model with greater initial capabilities and higher potential for future alignment tasks compared to the standard SFT approach.

**Exploration Capability via Rollout Branching Factor (RBF).** Beyond task performance, we investigated the intrinsic exploratory capacity of models, a critical factor for successful reinforcement learning. We measure this using the RBF (Deng et al., 2025a), which quantifies the diversity of a model’s generation by counting the number of candidate tokens within the probability mass of top p (0.95) during decoding. A higher RBF signifies greater generation diversity and, consequently, a stronger capacity for exploration. As shown in Table 4, our DPO-based cold-start method yields a substantially higher RBF than the SFT baseline. This finding suggests that our approach cultivates a broader exploration space, which is highly beneficial for the subsequent RL phase, enabling the model to discover more diverse and potentially higher-quality solutions. This outcome highlights a key advantage of our method in preparing models for alignment.

## A.5 RELATED WORK

The application of RL has emerged as a highly effective method for enhancing the reasoning capabilities of large language models, with notable successes in the text-only domain such as DeepSeek-R1 (Guo et al., 2025), which leverages RLVR (Lambert et al., 2024; Guo et al., 2025). Inspired by these advancements, a substantial and rapidly growing body of research has begun adapting RL techniques for Vision-Language Models (VLMs). This has catalyzed a wave of “MLLM-r1” studies, all aiming to harness similar principles to unlock more advanced multimodal reasoning abilities. For instance, specific approaches include exploring the frontiers of multimodal reasoning with rule-based reinforcement learning in **MM-Eureka** (Meng et al., 2025), creating a stable and generalizable R1-style model with **VLM-R1** (Shen et al., 2025), and empowering smaller models using two-stage rule-based RL as seen in **LMM-R1** (Peng et al., 2025). Researchers have also demonstrated significant visual reasoning on non-SFT models with **R1-Zero** (Zhou et al., 2025), learned step-wise reasoning with **R1-VL** (Zhang et al., 2025a), and achieved data-efficient self-improvement using MCTS-guided sample selection in SOTA with less (Wang et al., 2025b). Furthermore, innovative methods seek to incentivize self-reflection with **VL-Rethinker** (Wang et al., 2025a), encourage “thinking with images” in **DeepEyes** (Zheng et al., 2025), or unify various visual tasks under a single RL framework as proposed in **One RL to See Them All** (Ma et al., 2025).

A crucial precursor to effective reinforcement learning is the “cold-start” phase, which initializes the model’s policy before the RL stage begins. The predominant strategy for this phase is SFT on high-quality instruction-response pairs, a foundational step adopted by many leading models to establish a strong baseline performance (Wei et al., 2025; Yang et al., 2025; Huang et al., 2025; Deng et al., 2025b). In parallel with refining cold-start methods, the prohibitive cost of human annotation has driven the field towards synthetic data generation. This approach often involves using powerful teacher models to distill vast amounts of data for training smaller student models. This trend is evident in a variety of techniques, such as synthesizing multimodal instruction data from a single image with **Oasis** (Zhang et al., 2025b), empowering models with reflection via collective Monte Carlo Tree Search in **Mulberry** (Yao et al., 2024), and enabling models to reason step-by-step with **LLaVA-CoT** (Xu et al., 2024). These data-centric strategies, including those used to generate data for models like **Vision-R1** (Huang et al., 2025), are vital for creating the rich, high-quality datasets needed to effectively train and align modern VLMs for complex reasoning tasks.

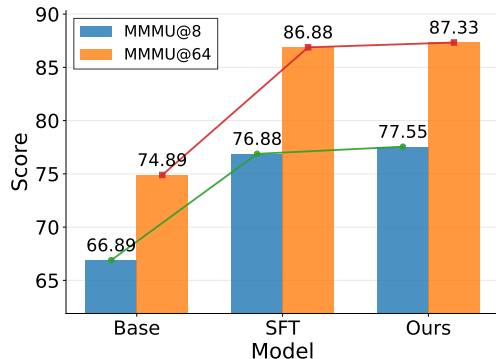
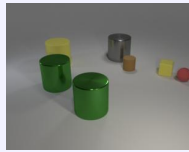


Figure 7: MMMU Pass@K Performance

## A.6 QUALITATIVE EXAMPLES

## QA Case Analysis: Case #001



**Question:** Hint: Please answer the question requiring an integer answer and provide the final value, e.g., 1, 2, 3, at the end. Question: Subtract all yellow matte blocks. Subtract all tiny brown cylinders. How many objects are left?

**Ground Truth:** 5

**Qwen2.5-VL-7B response:** 6

## Ours-7B response

<think>To solve the problem, first identify all objects in the image:

1. Yellow matte cylinder
2. Green metallic cylinder (left)
3. Green metallic cylinder (front)
4. Silver metallic cylinder
5. Tiny brown cylinder
6. Yellow matte block
7. Red matte sphere

Next, follow the instructions:

1. Subtract all yellow matte blocks: Removing the yellow matte block leaves 6 objects.
2. Subtract all tiny brown cylinders: Removing the tiny brown cylinder leaves 5 objects.

Thus, the remaining objects are 5.

</think>

<answer>The answer is 5</answer>

## Qwen2.5-VL-7B response

To solve this, we first identify all objects in the image: there are 8 objects in total. The yellow matte block is one object, and the tiny brown cylinder is another. Subtracting these two objects leaves us with  $8 - 1 - 1 = 6$  objects.

So, the number of objects left is 6.

### QA Case Analysis: Case #002

Web pages visited	
Person	Number of Web pages
Bonnie	84
Winston	56
Percy	70
Derek	68
Jake	60
Finn	47
Carter	75
Kurt	52

**Question:** Hint: Please answer the question requiring an integer answer and provide the final value, e.g., 1, 2, 3, at the end. Question: Several people compared how many Web pages they had visited. What is the mean of the numbers?

**Ground Truth:** 64

**Qwen2.5-VL-7B response:** 67.75

#### Ours-7B response

<think>To find the mean of the numbers, first sum all the numbers and then divide by the count of numbers.

The numbers are: 84, 56, 70, 68, 60, 47, 75, 52.

Sum of the numbers:

$$84 + 56 + 70 + 68 + 60 + 47 + 75 + 52$$

Calculating step by step:

$$84 + 56 = 140$$

$$140 + 70 = 210$$

$$210 + 68 = 278$$

$$278 + 60 = 338$$

$$338 + 47 = 385$$

$$385 + 75 = 460$$

$$460 + 52 = 512$$

The sum of the numbers is 512.

Next, count the number of values: There are 8 values.

The mean is the sum divided by the count:

$$\text{Mean} = \frac{512}{8} = 64$$

So, the mean of the numbers is 64.

</think>

<answer>The answer is 64</answer>

#### Qwen2.5-VL-7B response

To find the mean of the numbers, we need to follow these steps:

1. Add up all the numbers in the list.
2. Count how many numbers there are.
3. Divide the sum by the count.

Let's start with step 1: Add up all the numbers.

The numbers are: 84, 56, 70, 68, 60, 47, 75, 52.

$$\text{Sum} = 84 + 56 + 70 + 68 + 60 + 47 + 75 + 52$$

$$\text{Sum} = 542$$

...

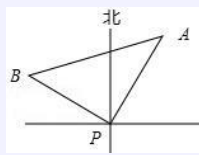
$$\text{Mean} = 542 / 8$$

$$\text{Mean} = 67.75$$

So, the mean of the numbers is 67.75.

**QA Case Analysis: Case #003**

**Question:** Hint: Please answer the question and provide the correct option letter, e.g., A, B, C, D, at the end. Question: At a certain moment, there is a passenger ship at sea point P, and lighthouse A is measured in the direction 30.0 north by east of P, and is 50.0 nautical miles away. The passenger ship sails at the speed of 60.0 nautical mile/hour in the direction of 60.0 from north by west for  $\frac{2}{3}$  hours to reach point B, then  $\tan \angle BAP =$



Choices:

- (A)  $\frac{4}{5}$  (B)  $\frac{6}{5}$  (C)  $\frac{\sqrt{5}}{5}$  (D)  $\frac{2\sqrt{5}}{5}$

**Ground Truth:** (A)  $\frac{4}{5}$

**Qwen2.5-VL-7B response:** (B)  $\frac{6}{5}$

**Ours-7B response**

<think>First, we need to determine the coordinates or distances relevant to the problem. The initial position of the passenger ship is at point P, and it is 50 nautical miles away from lighthouse A in the direction 30.0 degrees north by east. The passenger ship then sails in the direction 60.0 degrees from north by west for  $\frac{2}{3}$  hours at a speed of 60 nautical miles per hour, reaching point B.

The distance PB can be calculated as follows:

$$PB = 60 \times \frac{2}{3} = 40 \text{ nautical miles}$$

The direction 60.0 degrees from north by west means that the angle  $\angle BPA = 30.0^\circ + 60.0^\circ = 90.0^\circ$ . Therefore,  $\triangle ABP$  is a right triangle with  $\angle BAP = 30.0^\circ$ . In a right triangle, the tangent of an angle is the ratio of the opposite side to the adjacent side. Here,  $\tan \angle BAP = \frac{BP}{AP}$ .

Since  $AP = 50$  nautical miles and  $PB = 40$  nautical miles, we can use the Pythagorean theorem to verify:

$$AB = \sqrt{AP^2 + BP^2} = \sqrt{50^2 + 40^2} = \sqrt{2500 + 1600} = \sqrt{4100} = 10\sqrt{41}$$

However, we only need the ratio  $\frac{BP}{AP}$ :

$$\tan \angle BAP = \frac{BP}{AP} = \frac{40}{50} = \frac{4}{5}$$

Thus, the answer is [A].</think>

<answer>The answer is [A]</answer>

**Qwen2.5-VL-7B response**

To solve this problem, we need to determine the coordinates of points A and B relative to point P, and then find the tangent of the angle  $\angle BAP$ .

1. Determine the coordinates of point A relative to point P:

...

2. Determine the coordinates of point B relative to point P:

...

3. Calculate the tangent of  $\angle BAP$ :

... - Simplifying the expression, we get  $\frac{625\sqrt{3}-500-1250\sqrt{3}-1500}{625\sqrt{3}+1500-625\sqrt{3}+500} = \frac{-925\sqrt{3}-1000}{2000} = \frac{-925\sqrt{3}-1000}{2000} = \frac{-925\sqrt{3}-1000}{2000} = \frac{6}{5}$ .

Therefore, the correct answer is [B].